

Ion-Implanted Drift Field Silicon Solar Cell

Hee Yong Lee, Jin Kon Kim and Yoo Shin Kim

Korea Atomic Energy Research Institute, Seoul, Korea

(Recd. Jan. 23, 1976)

Abstract

An investigation on the effect of electrostatic drift field which can bring an additional aid to the photogenerated carrier collection in one side of the silicon solar cell has been carried out. The drift field was produced by the gradient of boron concentration in the p-type side in virtue of the strain compensation due to the tin dopant. A new method of ion implantation which is based on the principle of chiefly radiation-enhanced diffusion is adopted for forming the p-n junction in the solar cell. The open circuit voltage and the conversion efficiency of the ion-implanted silicon solar cell sample can be figured out to be 0.44 V and 5%, respectively.

요 약

시리콘 태양전지의 한쪽 면내에서 광에 의해서 발생된 전하운반체의 수집을 하는데 있어서 추가적인 도움을 줄 수 있는 정전적인 부동전계 효과에 관한 연구가 수행되었다. 주석(tin) 주입에서 오는 격자변형의 보상효과로 말미암아 P형 측내에 보론농도의 구배를 가져오므로서 부동전계를 발생시킬 수 있었다. 태양전지내에 p-n 접합을 형성시키기 위하여 주로 방사중식확산의 원리에 근거를 둔 새로운 이온주입법이 채택되었다. 이온주입으로 된 태양전지의 회로개방전압과 변환효율은 각각 0.44 V 및 5%였다.

1. Introduction

A number of investigations¹⁻³⁾ on the collection efficiency and spectral response of silicon solar cell have been carried out in recent years. The earlier investigators⁴⁻⁶⁾ have considered that the drift of minority carriers caused by an electrostatic field as an additional moving mechanism arises from gradient of the impurity concentration. The method of producing the drift fields in both sides of the silicon solar cell is in taking the

basic cell structure being either n^+-p-p^+ or p^+-n-n^+ . According to the literatures^{7, 8)} the principle of these structures is based on the theory of double injection of carriers into a semiconductor or an insulator.

Recently, Mandelkorn and Lamneck⁹⁾ have developed an efficient silicon solar cell having the cell structure of n^+-p-p^+ by diffusion process from both sides of the cell. More recently, Dalal, et al.,¹⁰⁾ have developed a very efficient silicon solar cell having the cell structure of epitaxially grown $n-p-p^+$ with the impurity density grading at

both n and p layers. Since the processes of forming these structures are very complicate, it may be mentioned that such expensive methods are not relevant in view of present tendency of producing the cheaper solar cells except the effort of academic interest to obtain high efficiency cells.

On the other hand, a simpler one side model such as the cell structure of p^+-p-n is desirable, but a breakthrough on the easier fabrication method than the conventional one is necessary. The present study is aimed at development of one side drift field silicon solar cell having the cell structure of p^+-p-n . This structure was formed by the gradient of boron concentration in the surface layer of the silicon substrate in virtue of simultaneous implantation with tin so as to cause the strain compensation. Although the photovoltaic power output of our lab.-made solar cell is a little lower than that of the commercial grade cell, it is certain that the very simple formation method of the $p-n$ junction will greatly contribute to this field.

II. The Enhancement Principle of Photovoltaic Power Output due to One Side Drift Field Silicon Solar Cell

(1) Energy Level Diagram

The dotted lines in Fig. 1-(a) show the energy level diagram of a shallow-doped ordinary $p-n$ junction in which each location of donor level (E_{dn}), acceptor level (E_{ap}), and Fermi level (E_F) is denoted. When the junction is irradiated by the sun-light, the energy level diagram is changed to the solid lines showing the formation of varied location of the Fermi level (E'_F), and the magnitude of the open circuit voltage (V_{oc}) is as shown in the diagram. It is generally

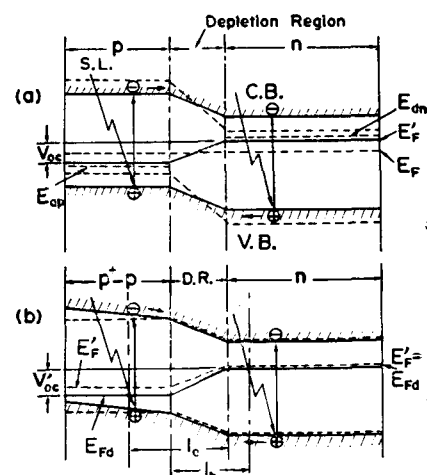


Fig. 1. Energy level diagrams of a shallow-doped ordinary silicon $p-n$ junction and the $p-n$ junction having a drift field in the one side

known that the open circuit voltage is proportional to the magnitude of difference of both Fermi levels between p and n regions.

When the p^+-p-n structure of silicon solar cell is irradiated by the sun-light, the varied energy level diagram can be illustrated as the solid lines of the Fig. 1-(b). As the convenience of illustration, the p^+-p region is denoted by a linear gradient of the doping level due to a single slope in each band edge in Fig. 1-(b), although the slope in the p^+ -region should be steeper than that in the p-region. The grading of the energy level with constant energy gap is combined with varied doping level in such a way that one side drift field will aid the collection normally carried by diffusion of the photogenerated electron-hole pairs. A high collection efficiency would require an extremely shallow p^+ -layer thickness having a high impurity concentration with each large average value of electron mobility and of electron lifetime.

As shown in the p-side of Fig. 1-(b), the

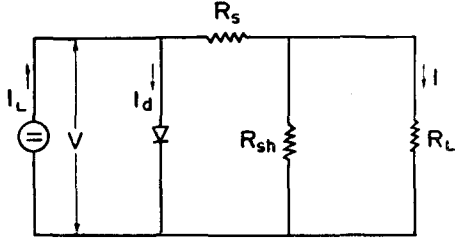


Fig. 2. Equivalent circuit of the silicon solar cell

drift field due to proper impurity grading can cause a varied position of the Fermi level (E_{Fd}), hence it can be seen that higher open circuit voltage (V'_{oc}) is produced in comparison with the case of Fig. 1-(a). The drift fields produced in both sides of a silicon solar cell should be more effective than one side model, but such a forming technique is very complicate, so that one side model is adopted in this study. The energy level diagram of irradiated state in Fig. 1-(a) is drawn in Fig. 1-(b) as the dotted lines for the comparison. The l_e and l_h in Fig. 1-(b) show the diffusion length of electron and that of hole for minority carriers, respectively.

(2) Measures for Power Output Enhancement

The equivalent circuit of a junction type silicon solar cell is shown in Fig. 2. When the Kirchhoff's first law is applied to the circuit, load current I flowed through the external load resistance R_L can be given as

$$I = I_L - I_d - \frac{V}{R_{sh}} \quad (1)$$

$$I_L = \beta q N_{ph}$$

$$I_d = I_o \left[e^{\frac{q}{AkT}(V+I \cdot R_s)} - 1 \right]$$

where I_L is the photogenerated current, I_d the forward current in the p-n junction, V the photogenerated voltage, R_{sh} the shunt resistance, β the collection efficiency, q the

electronic charge, N_{ph} the number of effective photons, I_o the reverse saturation current, A the factors due to crystal defect, k the Boltzmann's constant, T the absolute temperature, R_s the series resistance. The magnitude of I_L can be dominated by the values of β and N_{ph} .

If the term V/R_{sh} is neglected, I can be represented as

$$I = I_L - I_o \left[e^{\frac{q}{AkT}(V+I \cdot R_s)} - 1 \right] \quad (2)$$

when the circuit is open ($I=0$, $V=V_{oc}$), the open circuit voltage is given as

$$V_{oc} = \frac{AkT}{q} \ln \left(\frac{I_L}{I_o} + 1 \right) \quad (3)$$

and in case of short circuit current (I_{sc}) ($V=0$, $I=I_{sc}$), I_{sc} can be given as

$$I_{sc} = I_L - I_o \left(e^{\frac{q}{AkT} \cdot I_{sc} \cdot R_s} - 1 \right) \quad (4)$$

and if R_s is negligibly small, I_{sc} becomes equal to I_L .

In order to enhance the each value of I , V_{oc} , and I_{sc} in the relations (2), (3), and (4), the principal factors A and I_o should be minimized in view of physical properties of the solar cell. The A value which is caused by the state of crystal defect is generally limited in the scope of $3 > A \geq 1$ in a good solar cell. The I_o can be represented as

$$I_o = Sq n_i^2 \left(\frac{l_e}{\tau_e N_a} + \frac{l_h}{\tau_h N_d} \right) \quad (5)$$

where l_e and l_h are the diffusion lengths of minority carriers, τ_e and τ_h the average lifetimes of minority carriers, N_a and N_d the majority carrier densities, S the area of the p-n junction, and n_i the photogenerated intrinsic carrier density.

As the conditions of minimizing the I_o in the relation(5), each value of l_e and l_h is smaller the better while each value of τ_e , τ_h , N_a , and N_d is larger the better. As each of these minority carrier diffusion length is

defined as $l = (D\tau)^{1/2}$, $D = \mu kT/q$ (D , τ , and μ : diffusion coefficient, lifetime and mobility of minority carriers, respectively), l_e should be larger than l_h , because μ_e is fairly larger than μ_h in the silicon crystal at an ordinary given temperature. Since the thickness of p-layer is very thin (generally, less than $1\mu\text{m}$) in the p-on-n type cell, l_e should be limited within this thickness, and the ratio of l_e by l_h can be determined by that of μ_e by μ_h (l_e is about 2.5 times longer than l_h if the τ_e and τ_h are normal).

In proportion as the increase of N_a and N_d , τ_e and τ_h are to be decreased, and the most difficult problem of making a silicon solar cell is in such a puzzle. The best way of obtaining the necessary values of N_a and N_d without decreasing those of τ_e and τ_h is in increasing the velocity of each minority carrier by drift fields produced in both sides of the silicon solar cell.

In case of one side drift field model of p⁺-p-n structure to be dealt with in this article, since the carrier mobility is generally decreased in proportion to the increase of carrier concentration in the silicon crystal, the μ_e is gradually increased in accordance with the gradual decrease of N_a toward the junction boundary. As we know in the relation $v = \mu E$, the electron velocity is equal to the product of the electron mobility and an

electrostatic field strength. Hence, in the p-side, the electron (minority carrier) velocity should be proportionally increased in accordance with the gradual increase of μ_e at the presence of nearly constant value of the drift field due to the nearly linear gradient of N_a toward the junction boundary. The variable electron velocity means the acceleration of electron moving to compensate the decrease of τ_e without increasing the I_s in the equation (5).

III. Experimental

(1) Brief Description of the GDH-Implanter

The p-n junction having the p⁺-p-n structure for one side drift field silicon solar cell has been formed by the GDH (Gas Discharge and Heating)-Implanter which was developed by one of the authors.

The schematic illustration of the implanter is as shown in Fig. 3. A dopant-deposited silicon substrate which is placed underneath the grid type cathode is to be energetically bombarded by the neutralized heavy ions of argon gas under the preheating of the substrate, thus the dopant atoms can be implanted into the substrate by the processes of chiefly radiation-enhanced diffusion¹¹⁾ and of partly hot implantation¹²⁾. According to the literature¹³⁾, the target materials are not sputtered when the temperature of ma-

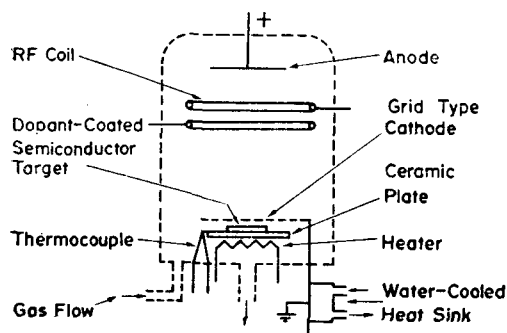


Fig. 3. Schematic illustration of the GDH-Implanter

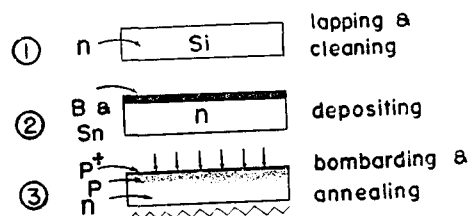


Fig. 4. Forming processes of the p-n junction having p⁺-p-n structure

materials is above 300°C. The detailed description of this implanter will be found elsewhere¹⁴⁾.

(2) Processes of Forming the p-n junction (p⁺-p-n structure)

An n-type silicon substrate having the crystal orientation of $\langle 100 \rangle$ and the resistivity of around 7Ωcm was cut into the size of 1 cm × 2 cm. The cut substrates were chemically etched by 4-1-1 etching solution (HNO₃:4, HF:1, CH₃COOH:1) for 2 minutes so as to take off the surface defects. Various pretreatments for the aid of cell fabrication are to be mentioned in Part III-(3). Both surfaces of the substrates were cleaned by acetone and trichloroethylene in turn with an ultrasonic cleaner, and washed fully by deionized water. The drying was done by a centrifuge with an aid of forcibly blown hot air of about 70°C. The forming processes of the p-n junction (p⁺-p-n structure) for one side drift field silicon solar cell are as illustrated in Fig. 4. The boron and tin were deposited on the silicon substrate in turn by controlling the thickness of each material in a vacuum coater. The boron deposition was done by thermal decomposition of B₂O₃ mixed with about 20 weight percent of aluminum powder as a reducer.

The simultaneous implantation of boron

and tin was done by controlling the substrate temperature. The tin dopant plays a role of strain compensation for the dense boron implantation to be discussed in part IV-(1). Since the tin dopant is a neutral impurity in the silicon, it does not affect the formation of p-n junction. The p⁺-p region (this means that the gradual decrease of p-type dopant concentration from the surface toward the junction boundary) due to the boron dopant was formed chiefly by the role of tin dopant and partly by the controlled temperature of the substrate. After the implantation and annealing, the remnant layer on the substrate was etched away by hydrochloric acid. The conditions of the implantation and annealing are shown in Table 1.

(3) Processes of Fabricating the Silicon Solar Cell

In order to get a passivation of the edge surface and to protect the leakage at the edge, SiO₂ layer was deposited around the edge of the silicon substrate prior to deposit the p-type dopants on the substrate. Silicon dioxide layer was easily formed on the substrate by evaporating silicon monoxide in a vacuum coater with a low vacuum environment of around 10⁻⁴ Torr. Such a coating on the edge area was done by using a metal mask made of a thin copper plate. After forming the SiO₂ edge layer, another metal mask was used in hiding the SiO₂ layer for the depositing of two dopants.

The opposite side of the substrate was plated by nickel. This process was also done prior to deposit the dopants on the obverse side of the substrate. The nickel was plated by electrodeless nickel plating method¹⁵⁾. The p-side electrode was formed on the p⁺-type layer by vacuum coating of Au-Cu

Table 1. Implanting Conditions

D	C	V _{dc} (V)	I _{cur} (mA)	T _{sub} (°C)	t _{imp} (min)	T _{ann} (C°)	t _{ann} (min)	TH _c (Å)
B		1,000	30	500 450 400	1 2 4	750	5	280
Sn		//	//	//	//	//	//	80

D: dopants, T_{sub}: preheated substrate temperature
t_{imp}: implanting time, t_{ann}: annealing time

C: Implanting conditions, TH_c: coated thickness
T_{ann}: annealing temperature, I_{cur}: dc ion current
V_{dc}: dc voltage

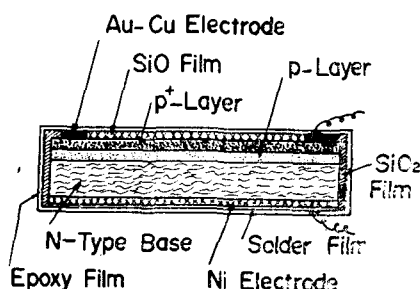


Fig. 5. Sectional view of the fabricated p^+ - p - n type silicon solar cell

alloy with a metal mask. Thin solder film was formed on the nickel film by vacuum coating.

The silicon monoxide thin film was formed on the p^+ -type layer as an antireflective coating. This coating was done by the evaporation of SiO with high vacuum environment of around 10^{-7} Torr. The leads for both electrodes were soldered by a low-melting-point solder. After finishing the soldering, transparent epoxy was coated on the whole cell by dipping it into the solution (epoxy #1500 solved with thinner) and dried

by hot air of around 70°C . The sectional view of the fabricated solar cell is as shown in Fig. 5.

IV. Results and Discussion

(1) Formation of the p - n junction (p^+ - p - n structure)

According to the literature¹⁵⁾, almost linear density gradient of boron formed from the surface toward the inside of the silicon bulk was obtained by the simultaneous diffusion of boron and tin. The solid solubility of boron in silicon can be easily exceeded in its critical limit by the strain compensation in the silicon lattice in virtue of the role of tin dopant. Since the TCR (tetrahedral covalent radius) of tin is larger than that of silicon, whereas the TCR of boron is smaller than that of silicon, it is thought that the silicon lattice, which would be expanded by tin atoms, counteracts the stress produced by the solute lattice contraction of the boron.

Since the doped profile of tin has a fairly large gradient of its concentration toward the inside of the silicon bulk in its diffusion as shown in Fig. 6, this effect has brought the gradient of boron concentration in the silicon bulk. A similar effect as the aforementioned can be expected in case of the simultaneous implantation of boron and tin in our lab.-made solar cell so as to bring the one side drift field as has been stated in Part II. The photomicrograph of the implanted profile in the cell is shown in Fig. 7. It is evident that the density gradient of the etch pits is caused by the gradient of boron concentration although the plastic deformation due to the solute lattice strain is greatly compensated by that of tin concentration.

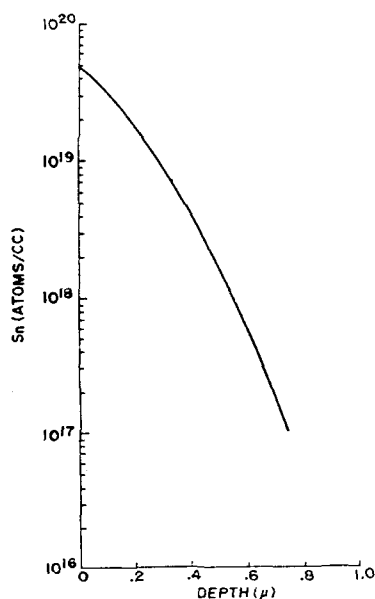


Fig. 6. Sn profile in presence of B diffused at 1200°C , 60 min (after Yeh and Joshi)

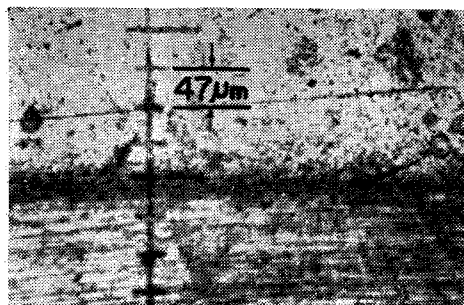


Fig. 7. Photomicrograph of the B+Sn-implanted p^+ - p - n type silicon p - n junction, which is delineated by HF-stain on the bevelled and lapped face with 3 degrees, $\times 160$

It is also certain that the fairly good photovoltaic effect (0.44 V) in the cell is caused by the formation of p^+ - p - n structure, although the concentrated degree in the p^+ -region of the cell is a little lower than that of an ordinary commercial grade cell having the surface impurity concentration of around 10^{19} atoms/cc. It has been already known that the photovoltaic effect of around 0.3V can be barely obtained by the merely shallow p - n junction in the silicon substrate without forming the gradient of the dopant concentration as has been explained of its reason in Part II-(1). The junction depth including the thinly doped p -region in our lab.-made solar cell sample as shown in Fig. 7 is around $1.2 \mu\text{m}$ and its surface concentration is around 3×10^{18} atoms/cc. Although we can not clearly identify the thickness of the p^+ -region (this is formed by the temperature control and the tin effect as shown in Table 1) through the photomicrograph shown in Fig. 7, it can be presumed through the density distribution of the etch pits that the thickness is around $0.5 \mu\text{m}$. It is known that the optimum junction depth of a silicon solar cell is generally formed within the range from $0.8 \mu\text{m}$ to $1 \mu\text{m}$.

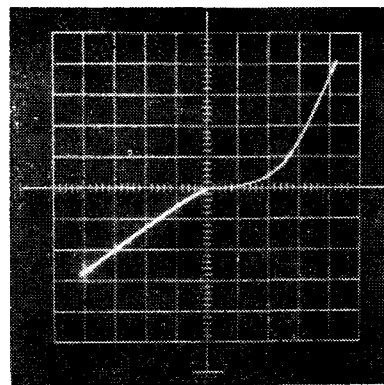


Fig. 8. I-V characteristics of our lab.-made silicon solar cell sample (sample(b)), Forward: 2 mA/Div., 0.2 V/Div., Reverse: 1 mA/Div., 1 V/Div., Active area: 0.48 cm^2

As has been stated in Part II-(2), the method of maximizing the N_a and N_d without decreasing each value of τ_e and τ_h in the silicon p - n junction for minimizing the I_o in the relation (5), special formation method should be taken in either double diffusion, n^+ - n - p^+ structure, or epitaxial growth for forming the very dense n^+ or p^+ -region. This is the main reason why the silicon solar cell is generally expensive. It is evident that our formation method is very simple in comparison with other conventional methods enabling the V_{oc} value of higher than 0.4 V.

(2) I-V Characteristics

In order to appreciate the physical state of the p - n junction in one of our lab.-made solar cells (B+Sn-implanted type, sample (b)), the I-V characteristics of the sample (b) as shown in Fig. 8 was compared with that of a commercial grade cell (B-double diffused type, made by KODENSHIKOGYO Co., Ltd. in Japan, sample (a)) as shown in Fig. 9.

The special feature of the forward curve shown in Fig. 9 is in almost straight rise

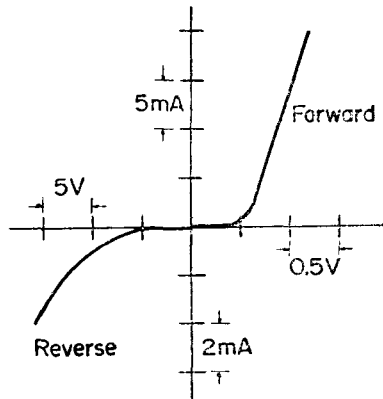


Fig. 9. I-V characteristics of a commercial grade silicon solar cell sample (sample (a)), Forward: 5mA/Div., 0.5V/Div., Reverse: 2mA/Div., 5V/Div., Active area: 0.6 cm²

except both a minor part of the exponential rise at the deflecting region and a flat part before the onset of the rise. This type of indication is often used when we measure the threshold voltage of a diode, so that such a form of the forward curve can be varied by changing the scales of current and voltage in a curve tracer. It can be thought that the threshold voltage of the forward current in a p-n junction is keenly related to both the diffusion lengths and average lifetimes of the minority carriers (I_s , I_h , τ_s , and τ_h).

As has been stated in Part II-(2), since the diffusion length and the diffusion coefficient can be defined as $l = (D\tau)^{1/2}$, $D = \mu kT/q$, each diffusion length of the minority carriers should be related to the average lifetime and average mobility of each minority carrier. Therefore, it can be said that the flat part is related to τ and μ whereas the straight part including the deflecting region is related to the diode equation

$$I_f = I_0(e^{\frac{qV}{kT}} - 1) \quad (6)$$

although the flat part is represented in the equation (6) subject to a small V-value and a little high A-value.

In order to get the larger values of τ and μ in the p-n junction of a solar cell, stronger built-in potential due to larger values of N_a and N_d in both p and n regions should be prepared as well as the stronger drift fields due to the gradients of both impurity concentrations. Generally, since the field due to built-in potential caused by the formation of charge neutrality is generally weaker than the drift field, it can be said that the flat part appears to be the case of the presence of a drift field. This fact can also be proved experimentally. When the p-n junction of a silicon solar cell is illuminated by a light, the flat part of the forward characteristic disappears, and such a disappearing effect is predominant in a good silicon solar cell. Under a light illumination to the sample (b), the flat part in the forward characteristic in Fig. 8 becomes to disappear as shown in Fig. 10.

This means that both flows of majority carriers and photogenerated intrinsic minority carriers are canceled each other as they have counter flowing directions as represented in equation (2) in case of $R_s = 0$ in Part II-(2). The canceled portion of the flat part can be added to the reverse curve under the light illumination. Such an effect should be a barometer in testing the quality of the silicon solar cell. The length of the flat part in Fig. 9 stands on the scale of around 0.5V whereas that in Fig. 8 corresponds to around 0.4V, i.e., the sample (b) has a little higher values of τ and μ than the sample (a). The higher threshold voltage means lower values of τ and μ regardless of the length of the flat part, but in case of the canceling due to a light illumination,

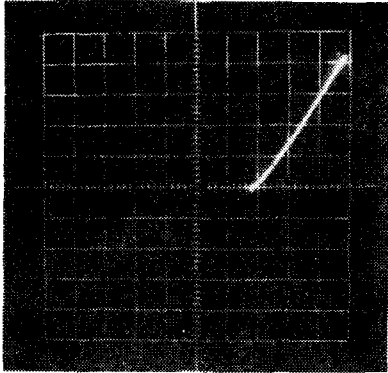


Fig. 10. Forward current characteristic of the sample (b) under a light illumination showing the disappearance of the flat part, Forward: 2 mA/Div., 0.2 V/Div., Active area: 0.48 cm²

the canceled portion of the flat part is nearly proportional to each magnitude of τ and μ values. Fairly large canceling effect shown in Fig. 10 means that the formation of the p-n junction having the p⁺-p-n structure is in tolerably good state as a silicon solar cell.

In the reverse characteristic of Fig. 9, it is showing a well-known "softness" in its curve. Such a softness can be obtained by a medium A-value ($3 > A \geq 1$) in the reverse current equation of a p-n junction. Generally, high A-value is caused by dense recombination centers. The reverse curve in Fig. 8 is showing a nearly straight line having somewhat ohmic characteristic. According to the literature¹⁷⁾, such an ohmic characteristic is caused by a little higher surface recombination velocity of the minority carriers. And it is also thought that the sample (b) has a little bumpy junction due to an insufficient impurity concentration whereas the sample (a) has a fairly good abrupt junction having a relevant impurity concentration. Generally, a fairly low reverse voltage is caused by a bumpy

junction having an insufficient impurity concentration. A little lower threshold voltage in Fig. 8 than that in Fig. 9 can be interpreted as the fact due to a little lower dislocation density in the sample (b) in comparison with that in the sample (a). Above canceling method is thought to be far simpler in checking the quality of a silicon solar cell than the method of checking the curve factor by a curve tracer.

(3) Efficiencies

Wolf¹⁸⁾ has classified the powerlosses which are related to the conversion efficiency. These are the following factors such as (a) reflection loss, (b) non-generative photon losses, (c) incomplete utilization of photon energy, (d) incomplete utilization of minority carriers, (e) surface and bulk recombination losses, (f) shunt and series resistance losses, and so on. Among these factors, the factors from (a) to (d) are chiefly dependent on the light absorption characteristic of the semiconductor material, which prescribes the short circuit current of a solar cell, and directly related to the over-all collection efficiency. The factor (e) is directly related to the I-V characteristics of the p-n junction, corresponding to the following items such as voltage factor relating to the open circuit voltage, the product of short circuit current by open circuit voltage, curve factor relating to the maximum derivable power output, and conduction mechanism of forward current in p-n junction in case of low impurity concentrations. The factor (f) is directly related to both the shunt leakage current and the series resistance due to both the bulk resistivity and the contact resistance.

If the measures for the utilization of sunlight are appropriate, the major part of the

Table 2. Estimation of the Maximum Expected Power Density of Each Sample due to the Measured Data under the Irradiation of Sun-Light

Samples	$V_{oc}(mV)$	$I_{sc}(mA/cm^2)$	$V_{oc} \cdot I_{sc}$ (mW/cm ²)	$0.8V_{oc} \cdot I_{sc}$ (mW/cm ²)	Conversion Efficiency at the Solar Radiant Power Density of 60 mW/cm ²
a	0.54	20	10.8	8.6	14.3%
b	0.44	8.3	3.7	3.0	5 %

power losses in a silicon solar cell can be governed by the factors (e) and (f). As has been discussed pertaining to the I-V characteristics of two different samples in Part IV-(2), the I-V characteristics of a silicon solar cell is a barometer of distinguishing the state of junction properties in the cell, hence the conversion efficiency is evaluated by the nature of the I-V characteristics of a silicon solar cell.

By analyzing the nature of I-V characteristics of a silicon solar cell, Prince¹⁹⁾ has derived a relation to calculate the rough estimation of the maximum expected power density as given below

$$P_A = 0.8V_{oc}I_{sc} \text{ Watts/cm}^2 \quad (7)$$

This relation is derived on the basis of his precise calculation in his previous work²⁰⁾, and is nearly correct at the conversion efficiency higher than 10.7%. We have roughly estimated the maximum expected power density of each sample by adopting the relation (7), and the results are shown in Table 2.

In the Table 2, both of V_{oc} and I_{sc} were measured under the direct irradiation of sun-light. Since the solar radiant power density is 100mW per square centimeter at sea level on a bright clear day with the sun at the zenith, reestimation of this value should be done, depending on the season and the latitude. The conversion efficiencies of the two samples were figured out by estimating the solar radiant power to be 60 mW per square centimeter at winter time

in Seoul. Since the conversion efficiency of present commercial solar cell (high grade) is generally 14.3% at the p-on-n type 1Ωcm silicon solar cell, our estimation in Table 2 may be almost reasonable.

The state of variation on each of V_{oc} and I_{sc} of the two samples per unit area were measured by varying the illumination intensity on each obverse face under an incandescent lamp, and the results are shown in Fig. 11 and Fig. 12. Observing each of V_{oc} and I_{sc} in both Figures, the sample (a) is fairly excellent and the sample (b) is a little poor. It is worthy to note that such a difference of the photovoltaic power in both samples are mainly caused by the different method of junction formation as has been stated in Part III-(2).

The maximum power output of the sample (b) through a matching load is yet in a little insufficient condition, since the electric contact due to the Au-Cu alloy on the

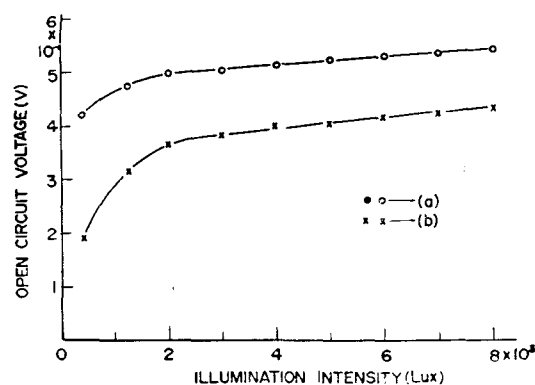


Fig. 11. Open circuit voltage vs. illumination intensity of each sample due to incandescent lamp

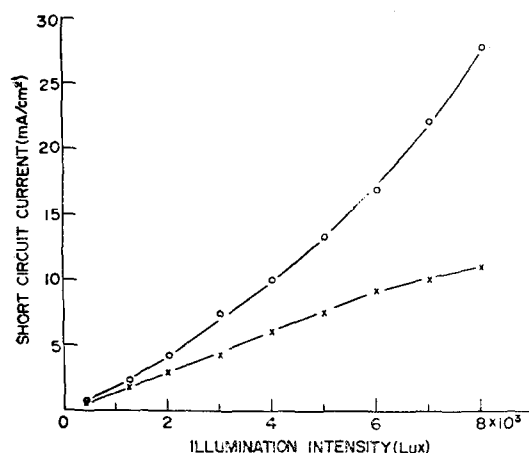


Fig. 12. Short circuit current vs. illumination intensity of each sample due to incandescent lamp

obverse p^+ -side is not enough on account of the difficulty of good cleaning on the densely doped surface and of irrelevant ohmic contact. And besides an alloy with cheaper materials than the gold alloy should be used. The nickel electrode on the rear n -side as a cheaper material can make a good electric contact by the electrodeless plating, and moreover nickel is an effective getter to the adsorbed gas and to preserve carrier lifetimes (Ref. 21) although the Schottky barrier height is fairly high (4.74 eV) (Ref. 22), but this type of n -side electrode can be used on account of its merits. Such a technique should be studied in detail in the further research.

V. Conclusion

The following conclusion can be drawn through the present research.

(1) The principle of the one side drift field model due to the p^+-p-n structure of the silicon $p-n$ junction for the solar cell was studied.

(2) The silicon $p-n$ junction having a gradient of dopant concentration was formed

in the newly developed GDH-Implanter without any trouble in its implanting mechanism.

(3) A gradient of implanted boron concentration in the p -type side of the silicon substrate was formed by the strain compensation in virtue of the tin dopant through the simultaneous implantation of boron and tin.

(4) A comparative analysis on the $I-V$ characteristics of our lab.-made sample and a commercial grade sample was done by contriving a simple method of checking the quality of silicon solar cell.

(5) The forming techniques of the $p-n$ junction in the high efficiency silicon solar cells having very dense dopant concentration in the p^+ -type surface layer are very complicate. This is the main reason why the silicon solar cell is generally very expensive. Although the open circuit voltage (0.44V) and the conversion efficiency (5%) of our lab.-made silicon solar cell are fairly lower than those of a commercial grade cell, it is noteworthy that the making processes of our cell are very simple than any other conventional methods. Recent tendency of developing the solar cells in the world is how to make a cheaper cell without making the most of its only high efficiency. Since we have developed a very simple and unique method of making the silicon solar cell by employing the GDH-Implanter, it is certain that this method will contribute to the earlier embodiment of the mass production of cheaper silicon solar cells not a little.

Acknowledgments

The authors would like to express their gratitude to Messrs. Chang Bae Moon and Sae Woo Jun for their helpful assistance throughout this research.

References

- (1) M. Wolf, Proc. IEEE 51 (5), 674 (1963).
- (2) R.V. Oberstraeten and W. Nuyts, IEEE Trans. ED-16 (7), 632 (July, 1969).
- (3) J.J. Loferski and J.J. Wysocki, RCA Rev. March 1961, p. 38.
- (4) W.R. Runyan and E.G. Alexander, IEEE Trans. ED-14 (1), 3 (Jan., 1967).
- (5) S. Kaye, IEEE Trans. ED-13 (7), 563 (1966).
- (6) M. Wolf, Proc. IRE 48, 1246 (July, 1960).
- (7) R. Baron, Phys. Rev. 137, A272 (1965).
- (8) J.W. Mayer, et al., Phys. Rev. 137, A286 (1965).
- (9) J. Mandelkorn and J.H. Lamneck, Jr., J. Appl. Phys. 44, 4785 (1973).
- (10) V.L. Dalal, et al., J. Appl. Phys. 46, 1283 (1975).
- (11) D.G. Nelson, et al., Applied phys. Lett. 15, 246 (1969).
- (12) T. Tokuyama, et al., OYO BUTURI, 6, 599 (1970).
- (13) F. Kloss and L. Herte, SCP and Solid State Technol. 10, 48 (Dec. 1967).
- (14) H.Y. Lee, J. Appl. Phys. (To be published in the June 1976 issue).
- (15) R. Proebsting, SCP and Solid State Technol. 7, 33 (Nov., 1964).
- (16) T.H. Yeh and M.L. Joshi, J. Electrochem. Soc. 116, 73 (1969).
- (17) H.E. Bridgers, et al. (ed.), "Transistor Technology", Vol. 1, p. 206, D. Van Nostrand Co. Ltd., Princeton (1959).
- (18) M. Wolf, Energy Conversion, 11, 63 (1971).
- (19) M.B. Prince, J. Appl. Phys. 26, 536 (1955).
- (20) M.B. Prince, Phys. Rev. 93, 1204 (1954).
- (21) W.J. Shattles and H.A.R. Wegener, J. Appl. Phys. 29, 866 (1958).
- (22) A.G. Milnes and D.S. Feucht (ed.), "Heterojunctions and Metal-Semiconductor Junctions", p. 164, Academic Press, New York & London (1972).